Low-temperature magnetization dynamics of oxygen-stabilized tetragonal Ni nanoparticles

Aparna Roy and V. Srinivas*
Department of Physics and Meteorology, Indian Institute of Technology, Kharagpur 721302, India

J. A. De Toro
Departamento de Física Aplicada, Universidad de Castilla–La Mancha, 13071 Ciudad Real, Spain

J. P. Goff
Department of Physics, University of Liverpool, Oliver Lodge Laboratory, Liverpool L69 7ZE, United Kingdom
(Received 20 September 2005; revised manuscript received 13 March 2006; published 5 September 2006)

A comprehensive study of the magnetization dynamics of oxygen-stabilized, tetragonal Ni (OS-Ni) nanoparticles (20 nm) prepared by the borohydride reduction method is reported. Both as-prepared and air annealed (at 573 K and 773 K) samples have been studied using ac susceptibility, aging experiments, and field cooled (FC) and zero field cooled (ZFC) magnetization measurements as a function of temperature. The OS structure, which is a deviation from the usual face-centered-cubic (fcc) structure of Ni, arises due to the presence of interstitial oxygen atoms in the unit cell of Ni and causes it to exhibit anomalous magnetic behavior such as a very large magnetization enhancement at low temperatures. Two low-temperature magnetic transitions in close succession, manifested in the form of a sharp peak at 20 K and a small hump at ~12 K, are observed in the ZFC curve and ac susceptibility plots of the as-prepared sample. The probable nature of these transitions has been explained on the basis of a model which associates the peak at 20 K with the occurrence of a PM (paramagnetic) → FM (ferromagnetic) transition of the oxygen-stabilized phase. Most of these newly formed FM particles block as soon as they gain internal order, yielding a strong irreversibility between the FC and ZFC branches. Some of the macromoments formed at 20 K, however, remain unstable down to 12 K, the temperature at which they block cooperatively as shown by a critical dynamics analysis, yielding critical exponent $z\nu = 9.84 \pm 0.48$ and a relaxation prefactor of $\tau_0 = 10^{-7}$ s. Aging experiments at 10 K for three different wait times t_w show wait time dependency, substantiating unequivocally the cooperative, chaotic nature of the sample magnetic dynamics. The low-temperature magnetic features displayed by the 573 K annealed sample closely resemble those of the as-prepared one, though distinctly different features are observed in the sample annealed at 773 K. These have been explained coherently taking into account the structural changes produced upon annealing.

DOI: 10.1103/PhysRevB.74.104402 PACS number(s): 75.75.+a, 75.40.Gb, 75.30.Kz, 75.25.+z

I. INTRODUCTION

The borohydride reduction technique is an indispensable and versatile method, widely used for the production of fine (3–200 nm) particles of ferromagnetic (FM) transition metals viz. Fe, Co, Ni, and their alloys in powdered form. First reported by Schlesinger and Brown,[1] this technique involves the reduction of transition metal salt solutions by an aqueous alkali metal borohydride—$NaBH_4$ or KBH_4—whereby the transition metal ions are brought to their metallic state. The resulting nanosized particles, apart from exhibiting a wide assortment of rich physical properties, may have potential applications in diverse areas such as magnetic recording media, sensors, ferrofluids and catalysts or may serve as model systems for understanding the dynamics of magnetization reversal process. However, the efficacy of their application will depend to a large extent on their thermal stability or their stability against oxidation and obviously on their magnetic attributes. A thorough understanding of the phase stability, oxidation kinetics, and the statics and dynamics of magnetization of magnetic nanoparticles prepared by the borohydride reduction method is therefore essential if they are to have any fruitful applications.

Surprisingly, however, there have been no systematic studies related to any of the above-mentioned aspects on samples produced by this technique. Some scattered but informative reports about the static magnetic properties of Co,[2] Fe-Ni-B,[3] and Co-Ni-B (Ref. 4) nanoparticles obtained by this method do exist in the literature, but there is still a lack of dynamical studies. One plausible reason for this could be the inherent uncertainty in the end product of the reaction due to the strong influence of preparation parameters on the composition, size, magnetic properties, and degree of crystallinity of the particles. For example, for Ni nanoparticles prepared by this method, no consensus could be reached regarding the compositional identity or the structure of the end product, obtained even under similar reaction conditions. While Glavee *et al.*[5] reported the formation of Ni and NiO when the reaction is carried out in aqueous medium and ambient atmosphere, Legrand *et al.*[6] after performing XPS (x-ray photoelectron spectroscopy) studies of their samples, reported that a mixture of Ni metal and Ni-B is formed under identical conditions. A rigorous magnetic characterization of samples prepared by the borohydride reduction method therefore needs to be preceded by a basic understanding of the reaction mechanism and a thorough investigation of two most important unexplored aspects of the end product—structure and phase stability.

Some attempts have been made in this direction by carrying out detailed structural and magnetic investigations on Ni

nanoparticles produced by this technique. Our choice of Ni stems from the fact that it has been a less studied metal in comparison to Fe and Co. Furthermore, most of the studies reported in the literature deal with complicated alloys[3,4] of this element in nanophase in which it is rather difficult to separate out various effects (impurity effects, surface effects, size effects) that contribute to the magnetic properties. A reaction mechanism for the formation of the Ni nanoparticles has been proposed and the crystallographic structure of the particles, which hitherto remained unidentified, has been identified. The reaction mechanism and structure identification has been discussed in detail in Ref. 7 where we have shown that Ni becomes stabilized in a tetragonal structure due to the incorporation of oxygen atoms in the Ni lattice. This structure—a deviation from the usual face-centered-cubic (fcc) structure of Ni—has been found to have a profound effect[8] on the static magnetic properties of the nanoparticles, involving some rich and unusual physics. The combination of "direct exchange" and oxygen-mediated "superexchange" interactions between the Ni atoms eliminates Ni ferromagnetism, yielding a paramagnetic state of tetragonal Ni at room temperature. The unusual physics lies in the combined use of these interactions, which points at the simultaneous display of two diametrically opposite behaviors—itinerant and localized—of the $3d$ electrons of a transition metal ferromagnet. Reference 8 reports a detailed discussion of these features in addition to an in-depth analysis of the thermal stability and an insight into the oxidation kinetics of the nanoparticles.

The magnetic studies reported in Ref. 8, mainly include an assessment of the room temperature (300 K) magnetic state of the oxygen-stabilized, tetragonal Ni (OS-Ni) nanoparticles (both as-prepared and annealed) on the basis of x-ray diffraction (XRD) and magnetization versus field (M-H) plots. However, some preliminary results on the thermal variation of magnetization (M-T plots) of these nanoparticles were also reported in the same reference. These clearly indicate the presence of a magnetic phase transition at 20 K in the as-prepared sample. Similar measurements on a series of samples prepared by the borohydride reduction of $NiCl_2$ solution of different molar concentrations ($0.1M-2M$) also show the presence of this low-temperature transition.[9] Hence the nature and origin of this transition, which is independent of sample molarity, needs to be investigated through a detailed dynamic study of magnetization of these samples. In this paper we report the low-temperature magnetization dynamics of one of these samples viz. $0.1M$, prepared by the borohydride reduction of $0.1M$ $NiCl_2$ solution.

II. EXPERIMENTAL DETAILS

Fine particles of Ni were prepared by reducing the nickel salt $NiCl_2 \cdot 6H_2O$ with sodium borohydride ($NaBH_4$) as the reducing agent. The details of the sample preparation can be found in Ref. 8. Furthermore, the structural (XRD) and microstructural [transmission electron microscopy (TEM)] characterization and measurements of phase stability [differential thermal analysis and thermogravimetric analysis (DTA and TGA)] of the samples have also been reported and analyzed in detail in the same reference. The particles have an average size of ~20 nm and their size is distributed over the range 15–26 nm. From the TGA curve, the atomic composition of the sample has been calculated to be $Ni_{54}O_{46}$, assuming the complete weight loss to be due to the desorption of the interstitial oxygen from the Ni lattice, which gives an upper bound for the oxygen concentration.

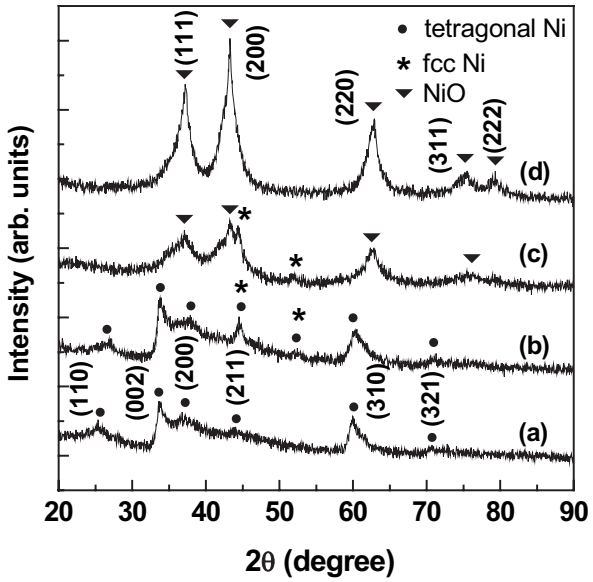

FIG. 1. X-ray diffractograms of as-prepared sample (a) and those annealed in air at (b) 573 K, (c) 773 K, and (d) 973 K for 1 h [Ref. 8]. The Miller indices corresponding to the peaks of tetragonal Ni are marked in Fig. 1(a) and those corresponding to NiO in Fig. 1(d).

The room temperature (RT) M-H curves were measured with a vibrating sample magnetometer using magnetic fields up to 14 kOe. The field cooled and zero field cooled (FC and ZFC) magnetization curves and the M-H curves at 5 K were measured with a commercial superconducting quantum interference device (SQUID) magnetometer (Quantum Design). SQUID magnetometry was also employed for recording ac susceptibility data (versus temperature and frequency of the applied field) in the frequency range 0.1 Hz–1000 Hz, with a field of amplitude 2 Oe. The aging experiment was performed in the same apparatus in the following way: the sample was first cooled from RT (300 K) down to the magnetically glassy regime. Then it was allowed to age for a waiting time t_w before applying a small external dc field ($H=10$ Oe) and registering the isothermal time evolution of the magnetization. This procedure was repeated for different t_w, keeping the same cooling rate.

III. RESULTS AND DISCUSSION

A. X-ray diffraction

The x-ray diffractograms of the as-prepared sample and those obtained after annealing in air at temperatures of 573, 773, and 973 K are shown in Fig. 1. The identification of the structure and indexing of the peaks of the diffractograms have been discussed in Ref. 8. The main points of the analy-

sis are (i) the as-prepared sample is oxygen-stabilized tetragonal Ni that is derived from the fcc Ni lattice by the incorporation of oxygen atoms at the interstitial positions of the latter. (ii) fcc Ni peaks appear on annealing in air at 573 K and more prominently at 773 K. (iii) Ni exists simultaneously in both fcc and oxygen-stabilized tetragonal phase in the 573 K annealed sample as portrayed by the diffraction pattern of this sample [Fig. 1(b)].

An inspection of Fig. 1 can offer qualitative information about the relative concentrations of the different phases in the samples. For example, in the as-prepared sample, the oxygen-stabilized tetragonal phase of Ni dominates over the fcc phase, with no detectable peaks of the latter in the XRD pattern. The situation is just the reverse in case of the 773 K annealed sample where fcc Ni dominates over OS-tetragonal Ni, with the XRD pattern not showing any discernable trace of the latter. On the other hand, in the sample annealed at 573 K the concentration of both phases is in the same order of magnitude, as suggested by the comparable peak intensities of these phases in the diffraction pattern of this sample. From these peak intensities, ignoring differences in the structure factors of the two phases, one may roughly estimate the fcc Ni volume fraction to be about 2/5 of that of tetragonal OS-Ni. A more rigorous quantitative estimation could be obtained with Rietveld refinement, which, however, is not indispensable for the discussion that follows.

B. Magnetic properties

As a prelude to our analysis of the magnetic state of the samples on the basis of magnetization versus temperature (*M-T*) curves and ac susceptibility plots, we enumerate below the salient features of the RT (300 K) *M-H* plots of these samples. Figure 2(a) shows the relevant plots. A nonsaturating hysteretic magnetization is observed for samples annealed in air, while very low magnetization values and a linear magnetization response with applied field is observed for the as-prepared sample, hinting at a paramagnetic (PM) state of this sample at 300 K. The complete analysis of different aspects of these plots along with a qualitative explanation of the paramagnetism of oxygen-stabilized tetragonal Ni (i.e., the elimination of Ni ferromagnetism by the oxygen in solid solution) and the low magnetization values have been proposed in Ref. 8.

Figure 2(b) shows the *M-H* plots of the as-prepared and the 573 K annealed sample at 5 K. Large values of magnetization, appreciably higher than the saturation magnetization of bulk fcc Ni (58.5 emu/g at 5 K) are observed. This magnetization enhancement along with hysteresis indicates some magnetic ordering at intermediate temperatures, the nature of which is discussed in Sec. III B 2.

1. Thermal variation of magnetization: Analysis of M-T curves

In order to gain more insight into the RT magnetic state of the samples, the *M-T* curves for all three samples were measured in zero field cooling (ZFC) and field cooling (FC) conditions under an applied field of $H=100$ Oe from 5 K to 200 K (Fig. 3). Figure 3(a) shows the FC and ZFC curves for the as-prepared sample. A perfect reversibility in the temperature range 70–200 K, followed by a rather faint bifurcation below 70 K is observed. With further decrease in temperature the ZFC curve shows a strong rise and finally merges with the FC curve at 22 K. This is followed by a pronounced bifurcation again at 20 K, with the ZFC curve forming a very sharp peak at this temperature before dropping towards zero. A small hump is seen in the ZFC magnetization at 12 K. Interestingly, the FC curve shows a peak at 19.5 K followed by a weakly temperature-dependent region. There are several reports[10–13] that dipolar interactions between particles can give rise to such a peak in FC magnetization. Also for certain of the canonical spin glasses, it is reported that a small peak develops with field cooling at T_f (freezing temperature),[14] followed by a plateau below it.

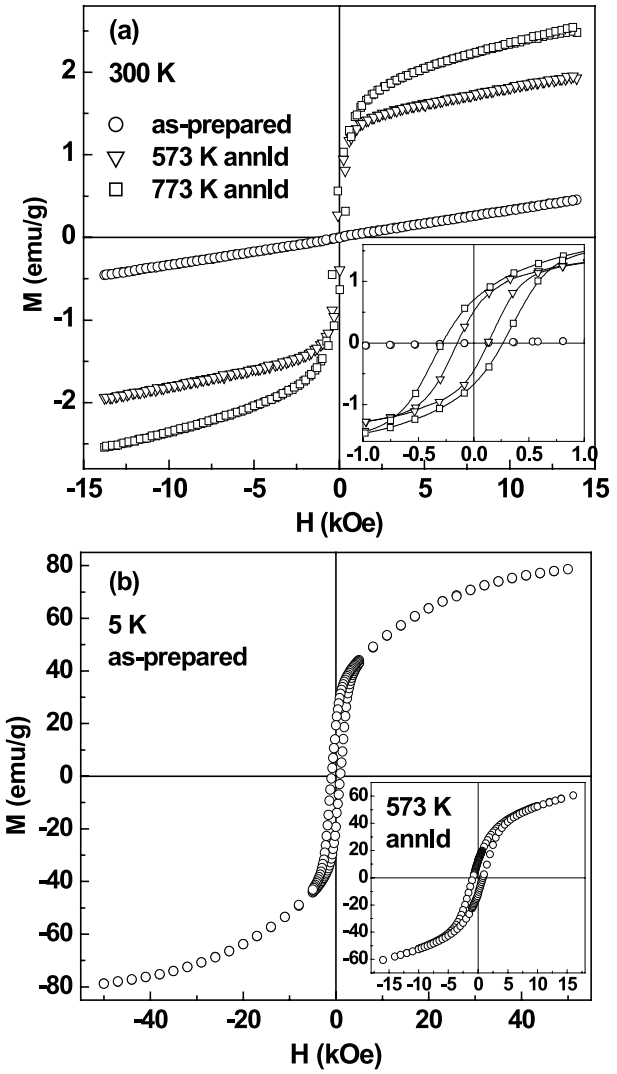

FIG. 2. (a) Magnetization (M) as a function of applied field (H) at 300 K for the as-prepared and annealed samples [Ref. 8]. Inset: An expanded view of the plots clearly showing hysteresis. (*b*) *M-H* plots at 5 K for the as-prepared and the 573 K annealed sample. For both samples, huge magnetization enhancement is seen at this temperature.

The complete reversibility in the temperature range 70–200 K (the starting temperature of the experiment) along with a linear magnetization response with applied field is

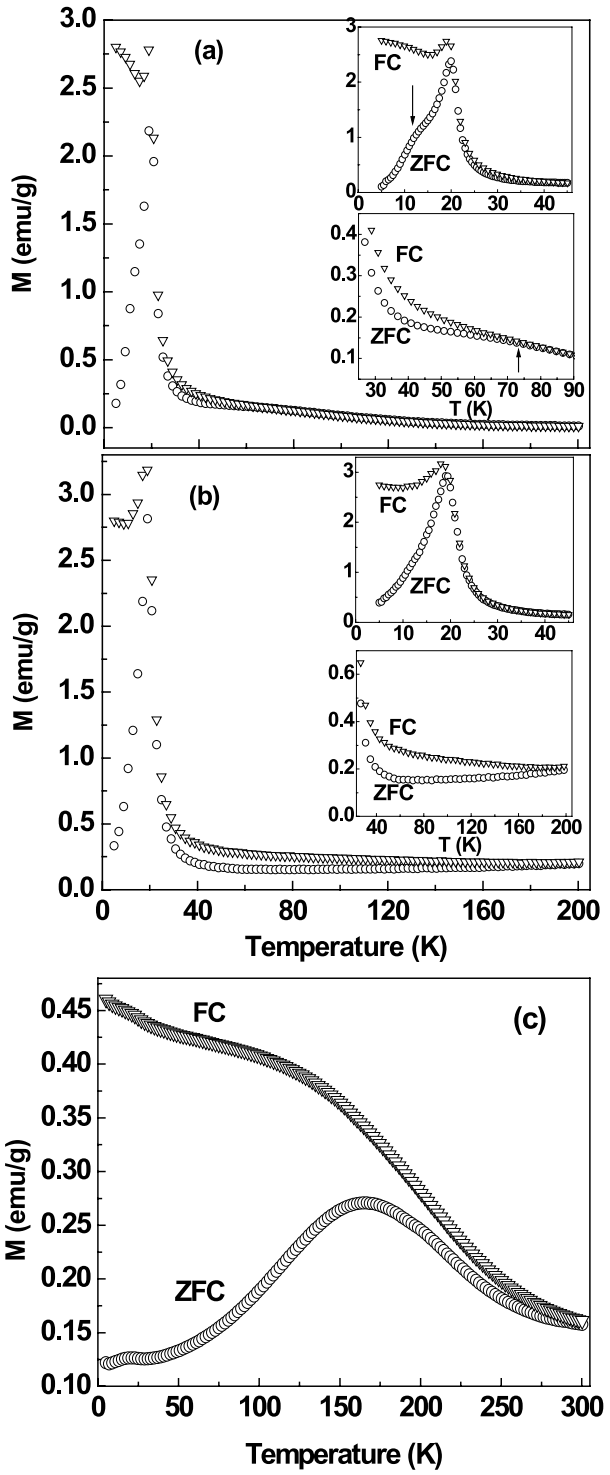

FIG. 3. Magnetization of FC and ZFC particles of (a) as-prepared, (b) 573 K annealed, and (c) 773 K annealed samples in 100 Oe applied field as a function of temperature. The insets in (a) and (b) focus on specific temperature ranges of the relevant plots for gaining a better perspective.

suggestive of a probable paramagnetic state of the particles at RT. However, the small deviation from reversibility at 70 K indicated by the faint bifurcation of these curves at this temperature, appears to be another magnetic anomaly that requires further investigation. Possibly it is due to the blocking of a few large particles containing a minority fcc phase, given the unavoidable distribution of particle sizes. These blocked particles are in no way representative of the sample. The strong rise of the ZFC curve, its merging with the FC curve, and the second bifurcation of these curves at 20 K is an indication of a transition to some low-temperature state. This will be analyzed in Sec. III B 2.

In contrast to the behavior displayed by the as-prepared sample, the FC and ZFC magnetization curves of the 573 K annealed sample show irreversibility right from the temperature of starting of the experiment (200 K) as evident from Fig. 3(b). This means that the particles, or more precisely, as explained below, the fcc Ni cores of the particles, absent in the as-prepared sample and still a minority phase here, are in a blocked state at 200 K (and probably at RT), with the FM hysteretic contribution to the magnetization response plotted in Fig. 2(a) being a manifestation of this state. The remaining low temperature features of the FC and ZFC curves, such as their merging at ~22 K and a second bifurcation at 20 K, are the same as those exhibited by the as-prepared sample. However, two minor points of difference are clearly seen. These include a perfectly flat, plateau-like FC magnetization below 20 K (absolutely no temperature dependence) and the absence of the small hump at 12 K.

A plausible reason for the difference in magnetic state of the as-prepared and the 573 K annealed sample could be the minority fcc Ni phase, which is found to start developing in the latter sample [Fig. 1(b)]. This means that this sample has Ni existing simultaneously in both tetragonal and fcc phases. Each particle, therefore, has a fcc Ni core surrounded by a major oxygen-stabilized tetragonal Ni part [Fig. 9(c) of Ref. 8]. The fcc cores, with their ferromagnetic alignment of spins, may be large enough—bearing in mind the size of the particles (20 nm) and the above estimated volume fraction of the fcc Ni phase—to be thermally stable. In addition, given they might have appreciably large moments, the subsequent dipolar interactions between them would enhance the effective anisotropy energy barriers and thus increase the blocking temperature. The observed hysteretic magnetization displayed by the 573 K annealed sample [inset of Fig. 2(a)] is a manifestation of the blocked state of these cores.

In contrast, the as-prepared sample, which has particles constituted only of tetragonal OS-Ni, behaves paramagnetically at RT, as evident from the linear magnetization response with applied field, and the value of the susceptibility $dM/dH=2.5\times10^{-5}$ emu/g Oe [as obtained from Fig. 2(a)], typical of a strong paramagnet. The paramagnetic nature of the OS-Ni at RT is certainly expected from the relatively high oxygen concentration in this phase. *Each particle of the as-prepared sample thus remains internally disordered with a paramagnetic collection of atomic spins within it*. It is seen from Fig. 2(a) that the sample annealed at 573 K also exhibits a PM component at RT, superimposed on the previously noted FM contribution. The PM component clearly has its origin in the major tetragonal OS-Ni phase of the particles where the oxygen in solid solution eliminates Ni ferromagnetism.

As regards the 773 K annealed sample, the FC and ZFC branches remain separated up to 300 K [Fig. 3(c)], which is the starting temperature of the experiment. A broad peak is

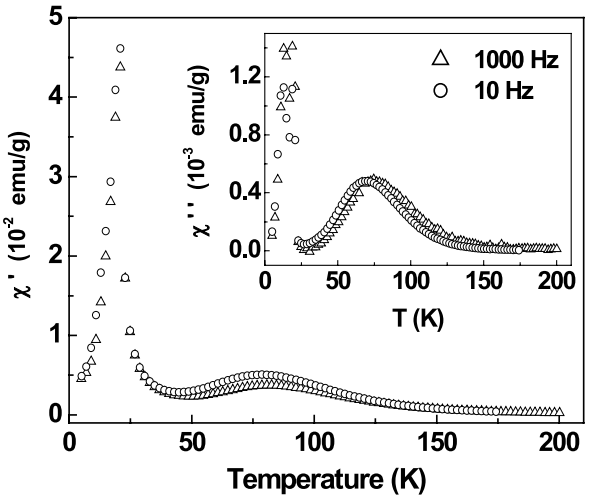

FIG. 4. Real (χ') and imaginary (χ'') components of ac susceptibility of the *as-prepared* sample measured as a function of temperature for two different frequencies, 10 Hz (O) and 1000 Hz (Δ) of the ac field (H=2 Oe). The temperature range 5–200 K includes the region of faint bifurcation (~70 K) in the FC and ZFC curves of this sample.

seen in the ZFC curve at 165 K instead of the sharp cusp at 20 K observed in the previous two samples. Recalling that the XRD pattern of this sample shows peaks of both NiO and fcc Ni, the peak at 165 K can be considered to signify the blocking of the superparamagnetic NiO shell (it is well known that nanoscale NiO is superparamagnetic) of the particles. On the other hand, the ferromagnetic component in the M-H loop at 300 K could stem from the blocked state of the fcc Ni cores of the particles [see Fig. 9(d) in Ref. 8 for a scheme of the structure of these particles].

2. Frequency dependence of ac susceptibility: Nature of the low-temperature transitions in the as-prepared sample

A preliminary idea about the existence of low-temperature magnetically metastable phases is obtained from the FC and ZFC magnetization curves shown in Fig. 3. However, a proper discerning of the nature of these phases and an understanding of the underlying physics leading to their occurrence requires dynamical tools like ac susceptibility experiments. This is a well-suited technique to characterize multiphase magnetic species, with the advantage that unlike the measurements of temperature-dependent magnetization, the results are independent of thermal history. Figure 4 shows the real (χ') and imaginary (χ'') components of linear ac susceptibility of the as-prepared sample, measured as a function of temperature for two different frequencies (10 and 1000 Hz) of the driving field of amplitude 2 Oe. Broad peaks seen at ~70 K, and the absence of a cusp or sharp maximum, are reminiscent of the progressive blocking of a few large particles, or particle Ni-rich cores, as mentioned in Sec. III B 1.

To unravel the significance of the peak at 20 K in the ZFC magnetization curve of the as-prepared and 573 K annealed samples, the ac susceptibility measurements for these samples were repeated for five different frequencies

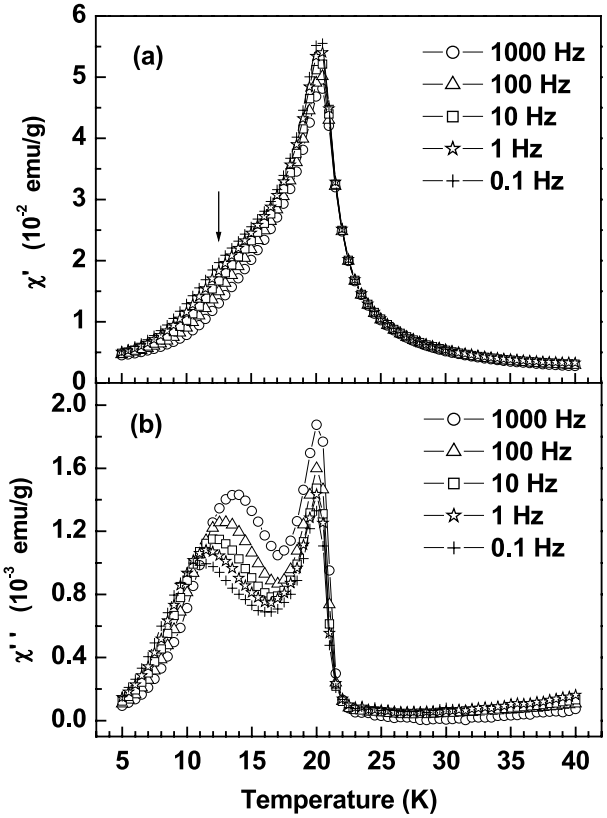

FIG. 5. Temperature dependence of real (a) and imaginary (b) components of ac susceptibility of the *as-prepared* sample measured at five different excitation frequencies. The temperature range 5–40 K encompasses the region of observation of the peak (~20 K) and the hump (~12 K) in the ZFC curve of this sample.

(0.1 Hz–1000 Hz) in the temperature range 5 K–40 K. Figure 5 shows these plots for the as-prepared sample. The sharp rise at 20 K from almost zero susceptibility as seen in both χ' and χ'' vs T plots is indicative of spin ordering at the atomic scale, most probably a Curie transition (PM to FM). This is confirmed by the near immobility of the peak temperature in χ' and χ'' with ac field frequency. It is clear that the phase responsible for the transition at 20 K is tetragonal OS-Ni, since the peak at this temperature is present in the M-T plots of the as-prepared and 573 K annealed samples, both comprising mainly tetragonal OS-Ni (paramagnetic at RT, as discussed above), whereas it has nearly disappeared or appears vanishingly small in the M-T plot of the 773 K annealed sample, which, as the XRD pattern shows, is constituted of NiO and fcc Ni but not tetragonal OS-Ni. We propose that the Curie-like PM to FM transition at T_C=20 K simply reflects the internal magnetic ordering of each particle, without the particles themselves being ferromagnetically aligned with respect to one another, i.e., the range of the FM order is limited by the particle size.

A pertinent question that needs to be addressed at this point is that if the transition at 20 K is to a FM-like state, why is there such a strong irreversibility below this temperature. Here is where the particle nature of the sample comes in. As soon as the particles develop magnetic order they become single-domain FM nanoparticles with a large moment.

If the Curie-like transition takes place under field cooling, the particle moments align between the field direction and their anisotropy axes, therefore yielding a net magnetization. If, however, the cooling through the transition is done in zero field the particle moments align randomly (and hence with very small net magnetization), as one may safely assume a random distribution for the orientation of the anisotropy axes of the particles. Irreversibility in the FC and ZFC curves thus begins as soon as the internal ordering of the particles has occurred. Upon heating, however, the peak at 20 K does not signal the deblocking of the particles, but a more radical change of scenario—the internal disordering of the particles to a PM state.

It is also apparent from Figs. 3(a) and 5(a) that in addition to the peak at 20 K, a hump is present at 12 K in the ZFC magnetization curve and in the χ' curves, indicating some supplementary effect or yet another phase transition. We interpret that not all the particle moments block at 20 K, as they are formed, but there must be an appreciable fraction of them, smaller or somehow isolated from the rest, that remain in a state of relaxation below this temperature, so as to finally undergo the transition at 12 K. Since the imaginary component χ'' of the linear ac susceptibility is the Fourier transform of the two-spin correlation function, it should show anomalous behavior near a magnetic transition. This is exactly what is depicted in the χ''-T plot [Fig. 5(b)], which shows prominent peaks in the vicinity of 20 K and 12 K, suggesting the occurrence of some relaxation phenomena at these temperatures. It will be shown that the transition at 12 K is the collective spin-glass-like freezing of the relatively small fraction of particles that remained unstable below the PM-FM transition at 20 K. It must be recalled that when interparticle dipolar interactions become appreciable compared to thermal energy, and given the anisotropic character of the dipolar interaction and the expected random position of the particles, they will provide the magnetic frustration[15] essential for the appearance of a glassy state. The hump at 12 K in the ZFC and χ' curves and the frequency dependence of the peak temperature near 12 K in the χ'' curves of the as-prepared sample thus point to the spin-glass-like (SGL) freezing of the particles at ~12 K, but with the atomic spin substituted by a particle "*superspin*." Such a particle collective state is sometimes known as *superspin glass*.[16] On application of a large magnetic field at 5 K, the superspins (both those blocking at 20 K and those freezing at 12 K) rotate from their frozen directions and align in the direction of the field, leading to the huge magnetization enhancement observed in the hysteresis loops measured at this temperature.

An important parameter widely used for quantitatively identifying a magnetic glass transition is Φ, defined as $\Phi = \Delta T_m / [\langle T_m \rangle \times \Delta \log_{10} f]$ (Ref. 14, p. 67), which gives the relative variation of the peak temperature T_m per decade of frequency f and is a simple approach to quantify the degree of interactions between magnetic moments. The parameter Φ for the transition at 12 K as deduced from the peak temperatures of the χ'' curves is 0.049 which is in the same range as found in metallic spin glasses and in the blocking of interacting particles,[17,18] and hence lends credence to our proposition of this transition being that to a magnetically glassy state.

A point to note here is that the FC magnetization of the as-prepared sample, in clear contrast to canonical spin glasses, does not exhibit any flat plateau below the transition temperature of 12 K but keeps increasing upon cooling, as in the case of superparamagnetic particles. This is because below 12 K the interaction strengths among the particles are somewhere between the two extremes of "very strong interaction" responsible for "infinite correlation" (perfect cooperative state) and "no interaction" responsible for "zero correlation" (individual relaxation). The particles interact strongly enough to yield a reduced frequency sensitivity of 0.049 but not strongly enough to develop an infinite correlation length. It is therefore quite probable that there is a distribution of correlation lengths, such that smaller correlated clusters of particles, or stray uncorrelated particles, block progressively in the field direction upon field cooling and give rise to an increasing magnetization signal. Thus the shape of the FC curve below 12 K in the as-prepared sample results from the sum of two contributions: (i) a flat portion originating from strongly correlated particles which blocked at 20 K immediately after gaining FM internal order (see next paragraph), and (ii) an increasing part superimposed on the former, stemming from the progressive blocking of the smallest particle moments (or of the clusters of particles with the weakest correlations) in the group of particles freezing at an average temperature of 12 K, as signaled by the hump in the ZFC curve. *We mention here that our use of the term "blocking" does not necessarily imply a "superparamagnetic blocking" of the particles. Rather the term is used in a broader sense to mean the "stabilization" of particle moments*.

Coming to the feasibility of the formation of a collective particle state immediately below 20 K, it may be recalled that the PM-FM transition at 20 K gives rise to an assembly of large enough magnetic moments in a rather high concentration. The resulting strong interparticle dipolar interactions and the random positioning of these particles suffice to create a collective spin-glass-like state below 20 K, right at the instant when the magnetic macromoments themselves are formed. This remarkable scenario explains the frequency insensitivity of the 20 K peak in ac susceptibility measurements: the peak shift, which is customarily detected when particle moments destabilize at a superspin-glass–superparamagnetic transition, is not observed in this case because the particles lose their internal magnetic order, i.e., the macromoments vanish or cease to exist before their thermal destabilization starts. *The Curie transition at* 20 K *therefore directly yields a superspin glass state at this very temperature*.

3. Aging phenomena and critical dynamics (as-prepared sample)

In order to probe the cooperative nature of the magnetic state of the as-prepared sample below the described transitions, aging experiments were performed at 10 K and 40 K. The former temperature is below and the latter is above these transition temperatures. The aging effect is usually observed in disordered spin systems governed by correlated dynamics and is related to the evolution of the spin-glass system within the characteristic multivalley free energy landscape. In the

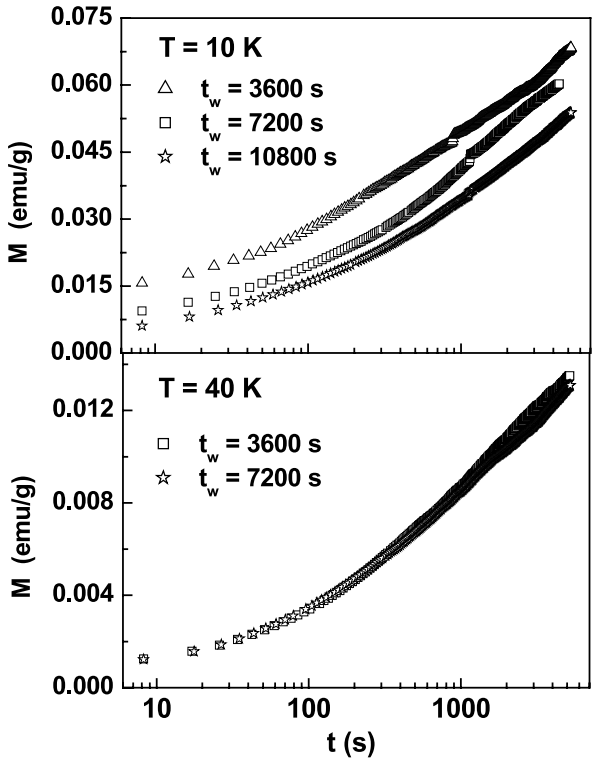

FIG. 6. Time dependence of the ZFC magnetization of the as-prepared sample measured at 10 K and 40 K for three different waiting times t_w before the application of a dc magnetic field $H=10$ Oe. A wait time dependence of ZFC magnetization is clearly apparent at 10 K while no such dependence could be resolved at 40 K in the experimental time window.

Fisher and Huse droplet model, a spin glass left unperturbed for a time t_w by external fields at a constant temperature T below the glass transition temperature T_g, rearranges its spin configuration spontaneously and continuously through a very slow process to reduce the domain wall energy (a domain can be thought of as a dynamic region of correlated spins). This makes the dynamics dependent on the time of wait t_w in the spin-glass phase after the quench from above the freezing temperature. Therefore the response to a small magnetic excitation after a waiting time of t_w is probing the polarization of the domains with different characteristic length scales. This wait time dependence of the magnetic response is weaker in magnetic particle systems as compared to that of an archetypal spin glass. The aging effect is an unequivocal sign of collective magnetic dynamics and vanishes at temperatures above the (super)spin freezing temperature.

Figure 6 exemplifies the magnetization (M) versus time (t) curves for the as-prepared sample measured at $T=10$ K and 40 K, for three different waiting times t_w as described in the experimental section. A small probing field of $H=10$ Oe has been used so that the sample is probed in the linear response regime. The curves measured at 10 K are clearly dependent on the elapsed time t_w before the application of the magnetic field H. This conclusively points at chaotic correlated dynamics. The usual decrease in magnetization with increasing t_w is also observed. As expected, the wait time dependency could not be resolved at $T=40$ K. It must be noticed that the observed aging behavior might be due both to the collective particle state formed immediately below 20 K, and also to the state developed by the interacting particles freezing at 12 K. However, the majority of the signal, as is clear from the inset of Fig. 3(a) (the hump seen in the inset is not a big feature and is contributed by a small fraction of the particles), comes from the former set of particles, and thus the aging behavior must in principle be attributed to them.

Concerning the functional dependence of $T_{max}(f)$ in the vicinity of 12 K, thermally activated dynamics laws of the Neél-Arrhenius type $[(\omega/\omega_0)=\exp(-E_a/K_BT)]$ could not fit the $T_{max}(f)$ data with physically meaningful parameters. The fit yielded unphysical values of 10^{20} Hz for ω_0 and 551 K for E_a/K_B. It has also been investigated whether the transition signaled by the peak at 12 K shows critical slowing down of the spin relaxation time. The dynamic scaling hypothesis states that the characteristic relaxation time close to the transition temperature is related to the spin-spin correlation length ξ, according to $\tau\sim\xi^z$. Since ξ diverges at the transition temperature according to $\xi\sim[(T/T_g)-1]^{-\nu}$, the relaxation time is expected to obey the temperature dependence

$$\tau=\tau_0\left[\frac{T}{T_g}-1\right]^{-z\nu}, \quad T>T_g,$$

where T_g is the static freezing transition temperature, τ_0 is the relaxation time of the individual (super)spins, ν is the critical exponent for the correlation length ξ, and z is the exponent relating the relaxation time $\tau(=1/\omega)$ with ξ. Substituting $T=T_{max}(f)$, where T_{max} are the frequency dependent peak temperatures at $\sim$12 K in the χ'' vs T plot, and $\tau=\tau_{measurement}=1/\omega=1/2\pi f$, a graph of log τ vs T_{max} can be plotted (f should be in Hz). Figure 7 shows the fit of the $T_{max}(\tau)$ data to the critical slowing down law for the spin relaxation time, with best fitting parameters $z\nu=9.84\pm0.48$, log $\tau_0=-7.14\pm0.27$, and T_g kept fixed at 9.5 K. The value of 10^{-7} s for τ_0 is too large compared to values usually derived for spin glasses. This can be explained by noting that in spin glasses τ_0 is determined by the spin flip time (10^{-13} s) of atomic magnetic moments, while τ_0 in a superspin glass transition is determined by the much larger relaxation time of the magnetic particles at the temperature where the transition takes place.[19] The value obtained for $z\nu$ lies well within the rather wide interval of values reported for 3D spin glasses.

C. Comparison of the magnetic properties of differently annealed samples

1. 573 K *annealed sample*

The 573 K annealed sample shows some dynamical features similar to the as-prepared sample, though a number of subtle differences are clearly discernable in the FC and ZFC curves [Fig. 3(b)] and ac susceptibility plots (Fig. 8). Coming to the similarities first, it is observed that the peak at 20 K is present in both M-T and ac susceptibility plots of both samples, with a virtually undetectable shift in the peak temperature with frequency in the latter measurements. Since the as-prepared sample is constituted only of OS-tetragonal

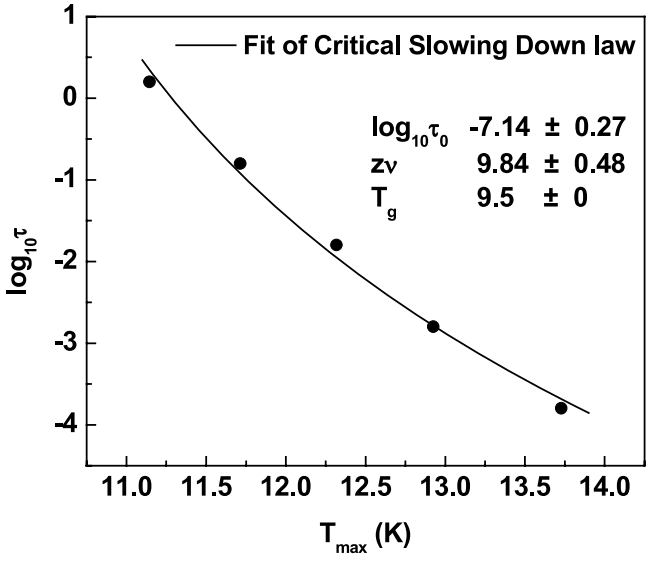

FIG. 7. Fit to the critical slowing down law for the relaxation time $\{\tau=\tau_0[(T/T_g)-1]^{-z\nu}\}$ of the as-prepared sample, performed using $T=T_{max}(f)$ where T_{max} are the peak temperatures at ~12 K in the χ'' vs T plot of this sample. The best fitting parameters are as indicated.

Ni and the 573 K annealed sample also has OS-tetragonal Ni as the majority phase, we can state without ambiguity that the peak at 20 K is due entirely to this phase. Hence the analysis of the 20 K transition as given in Sec. III B 2 is

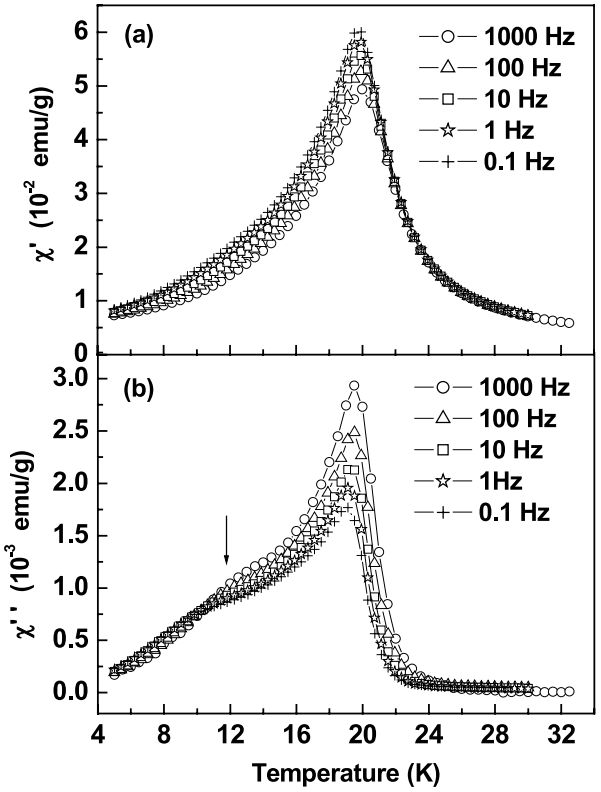

FIG. 8. Temperature dependence of (a) real and (b) imaginary components of ac susceptibility of the 573 K *annealed* sample, for different frequencies of the applied oscillating field.

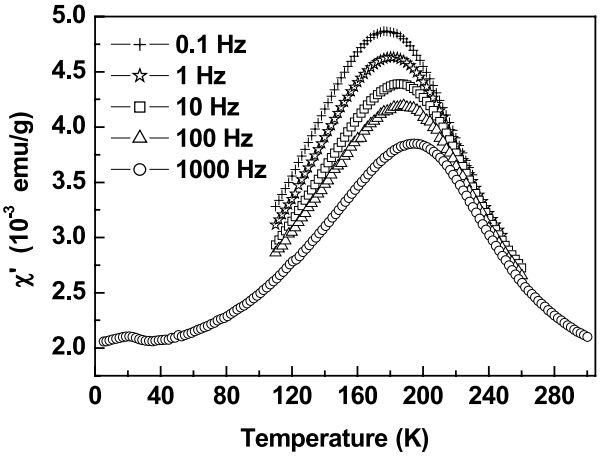

FIG. 9. Temperature dependence of the real component of ac susceptibility of the 773 K *annealed* sample, for different excitation frequencies.

applicable to the 573 K annealed sample as well.

As regards the differences, the hump at 12 K in the ZFC magnetization curve of the as-prepared sample is apparently missing in the 573 K annealed one. Correspondingly, the pronounced peaks at ~12 K in the χ'' vs T plot of the as-prepared sample are just in a rudimentary form here. Furthermore, the FC curve below 20 K is perfectly flat, in clear contrast to the increasing FC curve in the as-prepared sample. The disappearance of both the hump in the ZFC curve and the increasing signal (upon cooling) contribution to the FC magnetization suggest that both these features were due to the same fraction of particles, i.e., those still relaxing below 20 K (and blocking, on average, at 12 K) in the as-prepared sample. This fraction is negligible in the sample annealed at 573 K. This can be rationalized in terms of the larger Ni concentration in this sample, as evident from the presence of fcc Ni cores, and the subsequently stronger interparticle interactions, which would certainly make more unlikely the presence of the very small, isolated particles responsible for the 12 K transition. The flat aspect of the FC magnetization below 20 K in the 573 K annealed sample, and the absence of any hump in its ZFC curve in that region, can thus be understood simply as the result of subtracting the magnetic signal contribution (ii) described in Sec. III B 2, from the total magnetization of the as-prepared sample.

2. 773 K *annealed sample*

Distinctly different features in the form of broadened, dominant, peaks are observed in the ZFC magnetization curve [Fig. 3(c)] and ac susceptibility plots [Fig. 9] of the 773 K annealed sample. In addition, the peak at 20 K is present in just a hardly perceptible trace. This, as mentioned earlier, lends further credence to our proposition of the transition at 20 K being due to the tetragonal phase of Ni, which is paramagnetic at 300 K. It may be recalled that the 773 K annealed sample is constituted of NiO and the fcc phase of Ni in core (Ni)-shell (NiO) morphology with no discernable trace of the tetragonal phase. It is also observed from the *M-T* plot that the sample has a lower moment in comparison

to the as-prepared and 573 K annealed samples. This is because a significant portion of each particle is antiferromagnetic NiO [notice that antiferromagnetic (AFM) nanoparticles yield a low moment compared to FM particles, but still large enough—due to surface uncompensated spins—to produce superparamagnetic behavior].

The width of the peak in the ZFC curve and ac susceptibility plots is related to the size distribution of the magnetic particles undergoing the blocking. The parameter Φ calculated for this sample is 0.026, which is low compared to ideal superparamagnets and falls in the range of interacting particle ensembles. This can, however, be accounted for within the superparamagnetic framework by allowing a certain degree of interparticle interaction. Furthermore, the monotonous increase in the FC curve establishes the superparamagnetic-like behavior firmly. However, from an analysis of the frequency and temperature dependence of χ_{ac} it is logical to say that the sample exhibits a mixture of spin-glass-like and superparamagnet-like features, suggesting the picture of an ensemble of fine particles with strong interactions.

As mentioned earlier, the peak at 165 K in the ZFC curve of this sample has been attributed to the blocking of the superparamagnetic NiO shell of the particles. In order to confirm this, we further carried out *M-T* measurements on the 973 K annealed sample comprised of pure NiO nanoparticles [Fig. 1(d)]. For these particles, a blocking temperature $T_B \sim 120$ K was observed. The proximity of this 120 K peak to that at 165 K in the ZFC curve of the 773 K annealed sample, and the shape similarities between them, suggests that the transition at 165 K is due to the blocking of the NiO component of these particles. The difference in the T_B values of NiO in the 773 K and 973 K samples is probably due to the exchange coupling between the fcc Ni core and the NiO shell in each particle of the former sample. The exchange-bias effect can be used to increase the stability (blocking temperature) of FM particles surrounded by an AFM shell, as has been recently demonstrated.[20,21] The same arguments employed there, used in the opposite direction, can explain the stabilization of the net moment of AFM shells when they are exchange biased to a FM core. Exchange coupling is also manifest in the enhanced coercivity of this sample [see inset of Fig. 2(a)].

IV. CONCLUSION

The magnetization dynamics of fine Ni-based nanoparticles prepared by the borohydride reduction method have been investigated. From these investigations the following conclusions have been obtained: (i) The new crystal structure (tetragonal) arising from the incorporation of oxygen atoms in the unit cell of fcc Ni gives rise to anomalous magnetic behavior, such as a huge magnetization enhancement at low temperatures. (ii) The FC and ZFC magnetization curves and ac susceptibility plots reveal the occurrence of two magnetic transitions at 20 K and 12 K in the as-prepared sample and only the former transition in the sample annealed at 573 K. These low temperature transitions are due entirely to the structure and composition of the oxygen-stabilized tetragonal Ni nanoparticles. (iii) The features observed at 20 K in the ac susceptibility and *M-T* plots have been related to a PM to FM phase transition while those observed at 12 K have been attributed to the cooperative freezing of a minority fraction of macromoments that do not block immediately after the Curie transition. (iv) However, the majority of the moments that block immediately after the Curie transition, lead to the formation of a collective particle state at 20 K itself, i.e., right at the instant when the magnetic macromoments themselves are formed. The Curie transition at 20 K therefore directly yields a superspin glass state at this very temperature.

*Corresponding author. Fax: +91-3222-255303; Email address: veeturi@phy.iitkgp.ernet.in

[1] H. I. Schlesinger and H. C. Brown, J. Am. Chem. Soc. **75**, 215 (1953).
[2] J. P. Chen, C. M. Sorensen, K. J. Klabunde, and G. C. Hadjipanayis, Phys. Rev. B **51**, 11527 (1995).
[3] E. De Biasi, C. A. Ramos, R. D. Zysler, and H. Romero, Phys. Rev. B **65**, 144416 (2002).
[4] R. D. Zysler, H. Romero, C. A. Ramos, E. De Biasi, and D. Fiorani, J. Magn. Magn. Mater. **266**, 233 (2003).
[5] G. N. Glavee, K. J. Klabunde, C. M. Sorensen, and G. C. Hadjipanayis, Langmuir **10**, 4726 (1994).
[6] J. Legrand, A. Taleb, S. Gota, M. J. Guittet, and C. Petit, Langmuir **18**, 4131 (2002).
[7] Aparna Roy, V. Srinivas, S. Ram, J. A. De Toro, and J. M. Riveiro, J. Appl. Phys. **96**, 6782 (2004).
[8] Aparna Roy, V. Srinivas, S. Ram, J. A. De Toro, and U. Mizutani, Phys. Rev. B **71**, 184443 (2005).
[9] Aparna Roy, V. Srinivas, S. Ram, J. A. De Toro, and J. P. Goff, J. Appl. Phys. (to be published).
[10] J. L. Dormann, D. Fiorani, and E. Tronc, Adv. Chem. Phys. **XCVIII**, 283 (1997).
[11] R. W. Chantrell, N. S. Walmsley, J. Gore, and M. Maylin, J. Magn. Magn. Mater. **196-197**, 118 (1999).
[12] R. W. Chantrell, N. S. Walmsley, J. Gore, and M. Maylin, J. Appl. Phys. **85**, 4340 (1999).
[13] R. D. Zysler, D. Fiorani, and A. M. Testa, J. Magn. Magn. Mater. **224**, 5 (2001).
[14] J. A. Mydosh, *Spin glasses: An Experimental Introduction* (Taylor and Francis, London, 1993), p. 111.
[15] The random position and orientation of the macromoments causes the interactions among them to be randomly either ferromagnetic or antiferromagnetic depending on the relative orientation of each dipole. This fact stems from the expression $J_{ij}=\mu_i\mu_j(1-3\cos^2\theta_{ij})/r^3$, where J_{ij} is the strength of the interaction and θ_{ij} is the angle between the ith and jth dipole. Clearly, the sign of J_{ij} depends on θ_{ij}. The presence of these competing interactions

(FM and AFM) provides the "frustration" necessary for the appearance of a magnetically glassy state.

[16] J. A. De Toro, M. A. Lopez de la Torre, J. M. Riveiro, J. Bland, J. P. Goff, and M. F. Thomas, Phys. Rev. B **64**, 224421 (2001), and Refs. 3 and 8 therein.

[17] J. A. De Toro, M. A. Lopez de la Torre, J. M. Riveiro, A. Beesley, J. P. Goff, and M. F. Thomas, Phys. Rev. B **69**, 224407 (2004).

[18] J. L. Dormann, L. Besais, and D. Fiorani, J. Phys. C **21**, 2015 (1988).

[19] C. Djurberg, P. Svedlindh, P. Nordblad, M. F. Hansen, F. Bodker, and S. Morup, Phys. Rev. Lett. **79**, 5154 (1997).

[20] V. Skumryev, S. Stoyanov, Y. Zhang, G. Hadjipanayis, D. Givord, and J. Nogues, Nature (London) **423**, 850 (2003).

[21] J. M. Riveiro, J. A. De Toro, J. P. Andres, J. A. Gonzalez, T. Munoz, and J. P. Goff, Appl. Phys. Lett. **86**, 172503 (2005).